# ON THE SENSITIVITY OF MESOSCALE MODELS TO SURFACE-LAYER PARAMETERIZATION CONSTANTS

J. R. GARRATT* and R. A. PIELKE

*Dept. of Atmospheric Science, Colorado State University, Fort Collins, Colorado, 80523, U.S.A.*

(Received in final form 12 April, 1989)

**Abstract.** The Colorado State University standard mesoscale model is used to evaluate the sensitivity of one-dimensional (1D) and two-dimensional (2D) fields to differences in surface-layer parameterization "constants". Such differences reflect the range in the published values of the von Karman constant, Monin–Obukhov stability functions and the temperature roughness length at the surface. The sensitivity of 1D boundary-layer structure, and 2D sea-breeze intensity, is generally less than that found in published comparisons related to turbulence closure schemes generally.

## 1. Introduction

Use of first-order closure schemes for evaluating turbulent fluxes is common in many boundary-layer, mesoscale and general circulation models of the atmosphere. This involves a computation of eddy diffusivities throughout the boundary layer and, usually, application of Monin–Obukhov surface-layer theory for evaluating surface fluxes. This latter application involves some form of semi-empirical flux-profile formulation, with appropriate surface boundary conditions on wind, temperature and humidity, based on wind tunnel or atmospheric observations.

The comparison of numerical model fields with observations, and inter-model comparisons themselves, are crucial to the verification and acceptance of specific models and to the physical parameterization schemes used in the models. Recent model intercomparisons, and comparisons of planetary boundary layer (PBL) schemes within specific models, involving both first- and higher-order closures, have been described in the literature, e.g., by Clarke (1974), Mellor and Yamada (1974), Yu (1977), Manins (1982) and Mahfouf *et al.* (1987).

The present note describes the use of a particular mesoscale model to evaluate the sensitivity of computed model quantities and fields to values of surface-layer "constants" appearing in the specific surface-layer ensemble mean parameterization scheme.

## 2. The CSU Mesoscale Model

The Colorado State University (CSU) mesoscale model, in a number of modified versions, is being applied extensively around the world and uses Monin–Obukhov

* Corresponding Address: CSIRO Division of Atmospheric Research, Private Bag No. 1, Mordialloc, Vic. 3195, Australia.

*Boundary-Layer Meteorology* **48**: 377–387, 1989.

similarity theory to compute surface fluxes. A diagnostic surface energy balance (SEB) equation is utilized to evaluate surface temperature (c.g., Mahrer and Pielke, 1977; McNider and Pielke, 1981). In common with many numerical models, values of wind speed ($u_1$), potential temperature ($\theta_1$) and specific humidity ($q_1$) at any one time step and at the first atmospheric level (usually within the lowest 10% of the boundary layer), together with surface temperature and humidity ($\theta_0$ and $q_0$, respectively) computed at the previous time step, are used to update the turbulent parameters $u_*$, $\theta_*$ and $q_*$ (see below) by application of an iterative technique. The new flux values are then used to determine the new surface temperature, through an iterative solution of the SEB equation. In contrast, a modified version of the CSU model described by Arritt (1987) used a prognostic form of the SEB equation, and solved for the fluxes using the analytical scheme of Louis (1979).

Model results discussed in this note are based on the standard version of the model which uses the iterative surface-layer parameterization schemes described above.

## 3. Surface-layer Parameterization Schemes

### 3.1. Formulations

In the CSU model, and many others, the surface fluxes are related to the scaling parameters $u_*$, $\theta_*$ and $q_*$ through,

$$\tau = \rho u_*^2 , \tag{1}$$

$$H = -\rho c_p u_* \theta_* , \tag{2}$$

$$E = -\rho u_* q_* . \tag{3}$$

Here $\tau$ is the surface stress (momentum flux), $H$ is the sensible heat flux (positive during the day) and $E$ is the evaporation, all computed at a grid point and representing an ensemble average value. Use of the turbulent scaling parameters is at the very basis of the Monin–Obukhov theory, and these are related to mean field variables through the following,

$$u_* = \frac{k u_1}{\ln(z/z_0) - \Psi_M(z/L)} , \tag{4}$$

$$\theta_* = \frac{k \, \mathrm{Pr}^{-1}(\theta_1 - \theta_0)}{\ln(z/z_T) - \Psi_H(z/L)} . \tag{5}$$

A similar relation to (5) for $q_*$ can be written, with $\theta_1 - \theta_0$ replaced by $q_1 - q_0$. In the above, $k$ is von Karman's constant, Pr is a neutral turbulent Prandtl number, $z$ is height, $z_0$ and $z_T$ are aerodynamic roughness and temperature surface scaling lengths, respectively, and $L$ is the Monin–Obukhov stability length defined in terms of $u_*$ and $\theta_*$. Note that $\theta_0$ and $\theta_1$ are the values of potential

temperature at the height $z_T$ (not $z_0$) and a level usually several meters above the ground within the surface layer, respectively. Model schemes differ in their choice of $k$, Pr, $z_0/z_T$ and $\Psi_{M,H}$; our focus here is on the dependence of model results on values of these quantities when Equations (1) to (5) are used in the parameterization scheme. Some models use a free convection formulation for evaluating $H$ in unstable conditions so that the flux is independent of $u_*$ (e.g., Zhang and Anthes, 1982); others use the Louis analytical scheme (Louis, 1979) which replaces Equations 4 and 5 with,

$$u_*^2 = C_D(z/z_0, \mathrm{Ri}_B)u_1^2 \tag{6}$$

$$u_*\theta_* = \mathrm{Pr}^{-1}\, C_H(z/z_0, \mathrm{Ri}_B)u_1\Delta\theta\,, \tag{7}$$

where $C_D$ and $C_H$ are explicit analytical functions of a bulk Richardson number, $\mathrm{Ri}_B$, and $\Delta\theta = \theta_1 - \theta(z_0)$. Here $\theta(z_0)$ is the potential temperature at height $z_0$, and so may differ from the surface temperature $\theta_0$ if $z_T$ and $z_0$ differ.

The $\Psi$ functions in Equations (4) and (5) can be readily written in terms of the gradient function $\Phi$ discussed below.

### 3.2. Stability functions and $k$

The CSU model, together with many other models and schemes (e.g., Louis, 1979; Hansen *et al.*, 1983; Gross, 1985; Leslie *et al.*, 1985; Nickerson *et al.*, 1986), bases its surface-layer formulation on the observational results of Businger *et al.* (1971). Other models use an alternative set of constants, which differ primarily in the values assigned to $k$ and Pr (see below). The $\Psi$ and $\Phi$ functions are related by

$$\Psi = \int (1 - \Phi(\zeta))\, \mathrm{d}(\ln \zeta) \tag{8}$$

where $\zeta = z/L$. The $\Phi$ functions broadly take the form, for $\zeta \leq 0$,

$$\Phi_M = (1 - \gamma_1\zeta)^{-1/4} \tag{9}$$

$$\Phi_H = \mathrm{Pr}(1 - \gamma_2\zeta)^{-1/2} \tag{10}$$

and, for $\zeta > 0$,

$$\Phi_M = 1 + \gamma_3\zeta \tag{11}$$

$$\Phi_H = \mathrm{Pr} + \gamma_4\zeta\,. \tag{12}$$

Major results and review recommendations are summarised in Table I; for example, Dyer (1974) recommended the Businger-Dyer forms (see also Businger, 1988) with $k = 0.4$ or 0.41, $\mathrm{Pr} = 1$, $\gamma_1 = \gamma_2 = 16$, and $\gamma_3 = \gamma_4 = 5$. These values are supported substantially in later reviews by, e.g., Yaglom (1977) and Högström (1988). There is thus considerable evidence to suspect the values of $k$ and Pr found by Businger *et al.* (1971). Consequently, for an assessment of the impact

TABLE I

Values of surface-layer "constants" based on Equations (4) and (5) and (9) through (12) inclusive – from observations and the review of Dyer (1974). The Wieringa (1980) results are based on a re-analysis of the Kansas observations used by Businger *et al.* (1971)

| Source | $k$ | $Pr$ | $\gamma_1$ | $\gamma_2$ | $\gamma_3$ | $\gamma_4$ |
|---|---|---|---|---|---|---|
| Observations | | | | | | |
| W70 | – | – | – | – | 5.2 | 5.2 |
| DH70 | 0.41 | 1 | 16 | – | – | – |
| B71 | 0.35 | 0.74 | 15 | 9 | 4.7 | 4.7 |
| G77 | 0.41 | – | – | – | – | – |
| W80 | 0.41 | 1 | 22 | 13 | 6.9 | 9.2 |
| DB82 | 0.40 | 1 | 28 | 14 | – | – |
| W82 | – | 1 | 20.3 | 12.2 | – | – |
| H88 | 0.40 | 0.95 | 19 | 11.6 | 6.0 | 7.8 |
| Z88 | 0.40 | – | – | – | – | – |
| Review | | | | | | |
| D74 | 0.41 | 1 | 16 | 16 | 5 | 5 |

Sources as follows: W70 – Webb (1970); DH70 – Dyer and Hicks (1970); B71 – Businger *et al.* (1971); G77 – Garratt (1977); W80 – Wieringa (1980); DB82 – Dyer and Bradley (1982); W82 – Webb (1982); H88 – Hogstrom (1988); Z88 – Zhang *et al.* (1988); D74 – Dyer (1974).

of surface-layer "constants" on model quantities and fields, we choose to compare the standard CSU model formulation (which is based on the Businger *et al.* (1971) experimental results) with an alternative scheme, likewise based on high quality experimental results. We thus chose the data of Webb (1970, 1982), rather than e.g., the recommendations of Dyer (1974), with appropriate $\gamma$ values, $k = 0.4$ and $\mathbf{Pr} = 1$. This combination of constants approximates closely many of the results shown in Table I, but differs significantly from that of Businger *et al.* (1971).

### 3.3. The scaling length $z_T$

This parameter allows for the effect of the laminar sub-layer at a rough surface on the transfer of heat and moisture, relative to that for momentum; the ratio of $z_0$ to $z_T$ quantifies the excess resistance to the transfer of heat and water vapour relative to momentum. In the CSU model, allowance is made for this excess resistance; in many models it is not, e.g., Busch *et al.* (1976), Zhang and Anthes (1982), and any model using the scheme of Louis (1979) – e.g., Louis *et al.* (1981), Leslie *et al.* (1985).

The relationship between $z_0$ and $z_T$ for a range of natural surfaces was discussed by Garratt and Hicks (1973), with additional data presented in Garratt

and Francey (1978), and summarised in Brutsaert (1982). For a wide range in the roughness Reynolds number ($\mathrm{Re}_* = u_* z_0/\nu$, $\nu$ being kinematic viscosity) over land surfaces, they found

$$\ln(z_0/z_T) = 2.0\,. \tag{13}$$

Previously, wind-tunnel studies showed a strong dependence of $z_0/z_T$ upon the roughness Reynolds number, apparently related to the bluff, artificial nature of the surfaces used in the studies (Garratt and Hicks, 1973). Nevertheless, a modified form of this $\mathrm{Re}_*$ functional dependence was discussed by Zilitinkevitch (1970) for application in the real world, and subsequently used by Deardorff (1974) in his numerical study of the PBL (with a minor numerical constant modification). This is the relation used in the standard CSU model version, *viz.*,

$$\ln(z_0/z_T) = 0.13\,\mathrm{Re}_*^{0.45}\,. \tag{14}$$

In the usual $\mathrm{Re}_*$ range over land of 50–1000, Equation (14) is not too different numerically from Equation (13), which itself is representative of many natural surfaces, from bare soil through crops to forest canopies.

Model comparisons described herein use the standard model version with Equation (14) (results are indistinguishable when using Equations (13) or (14), as against adoption of the Reynolds analogy with $z_0 = z_T$).

## 4. Model Sensitivity to Surface-Layer Constants

We refer to the standard CSU model surface-layer parameterization scheme, using the results of Businger *et al.* and Equation (13) or (14) as Scheme 1. The alternative scheme based on Webb (1970, 1982) with $\gamma$ values as indicated in Table I, and with $k = 0.4$ and $\mathrm{Pr} = 1$, we refer to as Scheme 2; the standard scheme, with $z_0 = z_T$, we call Scheme 3. Results are based on a one-dimensional (1D) diurnal cycle over land, and a simple two-dimensional (2D) sea-breeze simulation.

In order to produce an intense sea-breeze circulation, and thus ensure maximum impact of changes to the surface-layer scheme on the sea-breeze simulation, we specified a dry surface – this maximises the sensible heat fluxes, and minimises evaporation, during the day. The case of a wet surface is thus not considered here, though in the 1D simulations one would expect similar behaviour in $q_*$ and $E$ as for $\theta_*$ and $H$ in the dry case.

### 4.1. 1-D DIURNAL CYCLE

Simulations were commenced at sunrise in midsummer for a latitude of 30° N, with a geostrophic wind of $5\,\mathrm{m\,s^{-1}}$ and an almost dry surface with a value of $z_0 = 0.05$ m. Surface humidity ($q_0$) was not calculated directly (e.g., through solution of a sub-surface moisture equation), but rather a surface wetness factor,

$m$, or ratio of actual to potential evaporation, was specified. We took $m$ as 0.05, giving midday Bowen ratios of about 5. Additional model runs not reported here showed that the main results were not sensitive to the values of geostrophic wind, surface wetness or roughness length. Differences between simulations were greatest near midday and we show in Table II relevant quantities for comparison, at $t = 6$ hrs and $t = 18$ hrs (midnight), including the mean boundary-layer temperature, $\hat{\theta}$. In addition, Figure 1 shows vertical $\theta$ profiles near midday, together with the time variation of mixed-layer depth as calculated directly in the CSU model using the prognostic relation of Deardorff.

Results can be summarised as follows –

(i) Differences between Scheme 1 ($k = 0.35$, Pr = 0.74) and Scheme 2 ($k = 0.4$, Pr = 1) are significant in both surface parameters and boundary-layer quantities. In Scheme 2, $H$ values are higher by about 15%, mainly the result of $u_*$ differences; the reason for this can be seen by reference to Equations (2), (4) and (5). Thus $u_*$ increases directly with $k$ ($\Psi_M$ is similar for the two schemes), whereas $\theta_*$ depends in a complex way on numerator and denominator in Equation (5). The corresponding differences in surface temperature reveal an inverse correlation with heat flux, the result of the computational method for $\theta_*$ and $\theta_0$. This follows from consideration of the SEB equation; at any time, the downward short and longwave fluxes can be taken as constant, $R$ (independent of $\theta_0$), so that the balance requires (for a dry surface),

$$H + \sigma\theta_0^4 + c(\theta_0 - \theta_b) = \text{constant} = R\,. \tag{15}$$

Thus any increase in $H$ (e.g., through $u_*$) requires a decrease in $\theta_0$. In the above, $\sigma$ is the Stefan–Bolzmann constant, $c$ is a soil thermal constant, and $\theta_b$ is a deep soil temperature.

The differences in $H$ values are reflected in differences in boundary-layer temperature and depth; Scheme 2 produces greater $H$, and hence greater PBL temperature and depth.

TABLE II

Comparison of surface parameters and mean boundary-layer temperature ($\hat{\theta}$) at $t = 6$ and 18 hrs of a 1D diurnal cycle ($t = 0$ corresponds to sunrise), for the three surface-layer schemes

| $t$ (hrs) | Scheme | $u_*$ (m s$^{-1}$) | $\theta_*$ (K) | $H$ (W m$^{-2}$) | $\theta_0$ (K) | $\hat{\theta}$ (K) |
|---|---|---|---|---|---|---|
| 6 | 1 | 0.30 | 1.24 | 451 | 314.7 | 296.2 |
| | 2 | 0.34 | 1.29 | 536 | 306.2 | 296.6 |
| | 3 | 0.30 | 1.40 | 514 | 308.7 | 296.5 |
| 18 | 1 | 0.10 | 0.12 | −16 | 288.8 | 299.3 |
| | 2 | 0.11 | 0.13 | −17 | 287.8 | 299.5 |
| | 3 | 0.11 | 0.13 | −17 | 288.1 | 299.4 |

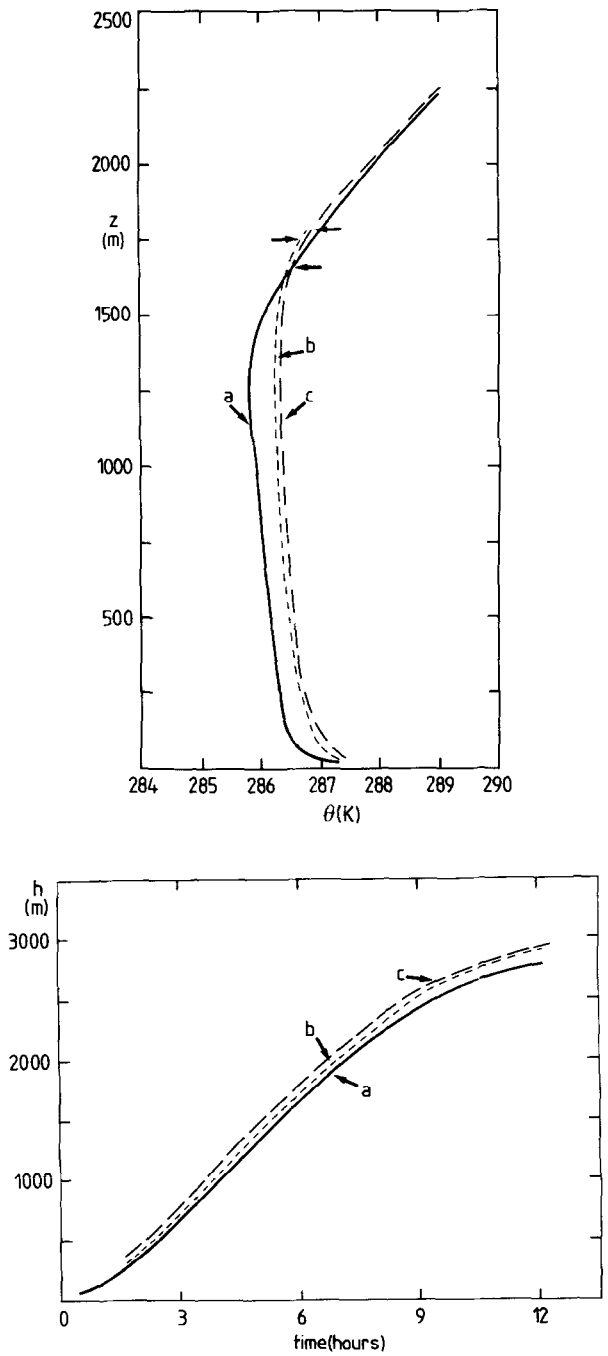


Fig. 1. (a) 1D potential temperature profiles at $t = 6$ hrs (near midday) for the three surface-layer schemes, as follows: curve a – scheme 1; curve b – scheme 2; curve c – scheme 3. Horizontal arrows indicate the boundary-layer top computed using Deardorff's prognostic equation. (b) Boundary-layer depth as a function of time for the 1D simulations and three surface-layer schemes.

(ii) Differences between Schemes 1 ($z_0/z_T \approx 7.5$) and 3 ($z_0/z_T = 1$) mostly affect thermal properties; during daytime, the results reveal the expected inequality – $\theta_0 = \theta(z_T) > \theta(z_0)$ when $z_T < z_0$ – with larger values of $H$ for the case $z_0 = z_T$ as result of increased $\theta_*$ alone. The friction velocity is unaffected. As before, boundary-layer properties change accordingly, so that use of the erroneous Reynolds analogy results in a daytime PBL that is too deep and too warm.

Nighttime results are relatively insensitive to changes in the surface-layer parameterization "constants".

### 4.2. 2-D SEA BREEZE

For these simulations, we took an $84 \times 20$ grid, $\Delta x = 7.5$ km, for latitude 30° N in summer with an offshore geostrophic wind of $5\ \mathrm{m\ s^{-1}}$ and sea-surface temperature of 290 K; the surface was almost dry ($m = 0.05$) with $z_0 = 0.05$ m. Table III gives the comparison details at $t = 9$, 12 and 15 hrs when the sea-breeze intensity (defined in terms of the maximum vertical velocity, $w_{max}$, at any one time) was near its maximum. Differences amongst the three schemes are directly the result of prefrontal differences in surface heat flux as determined in the 1D comparisons. Thus, the standard model version (Scheme 1) gives the smallest $H$ (and greatest $\theta_0$), lowest prefrontal PBL temperatures – therefore lowest cross-frontal thermal contrast – and smallest updraft vertical velocity. There is little significant difference in sea-breeze structure when either Schemes 2 and 3 are used, again consistent with 1D results if applied to the prefrontal situation. Any differences between schemes tend to diminish as the day progresses through sunset, so by $t = 15$ hrs when the lower atmosphere is stably stratified, the results in terms of $\hat{\theta}$ (which drives the circulation) are little different.

TABLE III

Comparison of surface parameters and mean boundary-layer temperature ($\hat{\theta}$) inland of a 2D sea breeze, together with maximum updraft velocity ($w_{max}$), for the three surface-layer schemes. Values are shown at three times, with $t = 0$ corresponding in sunrise.

| $t$ (hrs) | Scheme | $\theta_0$ (K) | $\hat{\theta}$ (K) | $H$ (W m$^{-2}$) | $w_{max}$ (m s$^{-1}$) |
|---|---|---|---|---|---|
| 9 | 1 | 315.8 | 298.6 | 407 | 0.38 |
| | 2 | 308.2 | 299.1 | 457 | 0.45 |
| | 3 | 310.2 | 299.0 | 449 | 0.47 |
| 12 | 1 | 306.7 | 300.0 | 133 | 0.45 |
| | 2 | 304.6 | 300.4 | 119 | 0.48 |
| | 3 | 304.5 | 300.4 | 126 | 0.51 |
| 15 | 1 | 293.2 | 300.1 | −21 | 0.38 |
| | 2 | 292.0 | 300.4 | −22 | 0.40 |
| | 3 | 292.1 | 300.4 | −22 | 0.41 |

## 5. Discussion

We find that uncertainties in surface and surface-layer parameterization "constants" affect mixed-layer temperatures by no more than about 0.5 K, and the mixed-layer depth by less than 200 m; nighttime surface temperatures are affected by less than 1 K. For a typical intense sea-breeze circulation over a nearly-dry surface, updraft velocities differ by about 0.1 m $s^{-1}$ at the most (for a grid length of 7.5 km). The sensitivity of boundary-layer structure to uncertainties in surface-layer parameterization "constants" is comparable with, but no greater than, that due to uncertainties in PBL eddy diffusivity (K) parameterization schemes. For example, Clarke (1974) compared a number of methods (mainly first-order K schemes of varying complexity) and found a range in daytime $u_*$ of about 0.24 to 0.31 m $s^{-1}$. Both Yu (1977) and Mahfouf *et al.* (1987) compared 1D boundary-layer structure under diurnal forcing using several K schemes, including that of O'Brien (1970) – used in the CSU standard version – and a turbulent kinetic energy approach. Yu (1977) – see his Figures 6 and 7 – found differences in boundary-layer temperature and depth during daytime of 1 to 2 K and 200 to 300 m, respectively; in contrast, Mahfouf *et al.* (1987) – see their Figure 2 – found smaller differences of 0.5 K and 50 to 100 m. In addition, Manins (1982) – see his Figures 2, 3, 6 and 7 – compared several similar schemes and found differences of less than 1 K and 200 m. Finally, in a set of 3D simulations, Mahfouf *et al.*'s (1987) sea-breeze comparisons produced a range in maximum vertical velocity of 0.10 to 0.17 m $s^{-1}$ for a horizontal grid length of 11 km – somewhat greater (in a relative sense) than values seen in Table III for a grid length of 7.5 km.

The results presented here should be applicable to other models that use Monin–Obukhov theory to determine surface fluxes from surface-layer variables. This should be so, irrespective of the complexity of schemes used to calculate, e.g., surface moisture (with sub-surface moisture fluxes and inclusion of vegetation), turbulent fluxes throughout the boundary layer, and the impact of sub-grid variability.

## Acknowledgements

The work reported in this paper was sponsored by the National Science Foundation (NSF) under grant number ATM86-1662. Computer calculations were made at the National Center for Atmospheric Research (NCAR). NCAR is sponsored by the NSF.

## References

Arritt, R. W.: 1987, 'The Effect of Water Surface Temperature on Lake Breezes and Thermal Internal Boundary Layers', *Boundary-Layer Meteorol.* **40**, 101–125.

Brutsaert, W.: 1982, *Evaporation into the Atmosphere*, D. Reidel Publ. Co., Boston, U.S.A., 299 pp.

Busch, N. E., Chang, S. W. and Anthes, R. A.: 1976, 'A Multi-level Model of the Planetary Boundary Layer Suitable for Use with Mesoscale Dynamic Models', *J. Appl. Meteorol.*, **15**, 909–919.

Businger, J. A., Wyngaard, J. C., Izumi, Y. and Bradley, E. F.: 1971, 'Flux-profile Relationship in the Atmospheric Surface Layer', *J. Atmos. Sci.*, **28**, 181–189.

Businger, J. A.: 1988, 'A Note on the Businger–Dyer Profiles', *Boundary-Layer Meteorol.* **42**, 145–151.

Clarke, R. A.: 1974, "Attempts to Simulate the Diurnal Course of Meteorological Variables in the Boundary Layer', *Izv. Atmos. Oc. Phys.* **10**(6), 600–612.

Deardorff, J. W.: 1974, 'Three-Dimensional Numerical Study of the Height and Mean Structure of a Heated Planetary Boundary Layer', *Boundary-Layer Meteorol.* **7**, 81–106.

Dyer, A. J.: 1974, 'A Review of Flux-profile Relationships', *Boundary-Layer Meteorol.* **7**, 363–372.

Dyer, A. J. and Hicks, B. B.: 1970, 'Flux-gradient Relationships in the Constant Flux Layer', *Quart. J. Roy. Meteorol. Soc.* **96**, 715–721.

Dyer, A. J. and Bradley, E. F.: 1982, 'An Alternative Analysis of Flux-gradient Relationships at the 1976 ITCE', *Boundary-Layer Meteorol.* **22**, 3–19.

Garratt, J. R.: 1977, 'Review of Drag Coefficients over Oceans and Continents', *Mon. Wea. Rev.* **105**, 915–929.

Garratt, J. R. and Hicks, B. B.: 1973, 'Momentum, Heat and Water Vapour Transfer to and from Natural and Artificial Surfaces', *Quart. J. Roy. Meteorol. Soc.* **99**, 680–687.

Garratt, J. R. and Francey, R. J.: 1978, 'Bulk Characteristics of Heat Transfer in the Unstable, Baroclinic Atmospheric Boundary Layer', *Boundary-Layer Meteorol.* **15**, 399–421.

Gross, G.: 1985, 'An Explanation of the "Maloja-Serpent" by Numerical Simulation', *Beitr. Phys. Atmosph.* **58**(4), 441–457.

Hansen, J., Russell, G., Rind, D., Stone, P., Lacis, A., Lebedeff, S., Ruedy, R., and Travis, L.: 1983, 'Efficient Three-Dimensional Global Models for Climate Studies: Models I and II', *Mon. Wea. Rev.* **111**, 609–662.

Högström, U.: 1988, 'Non-Dimensional Wind and Temperature Profiles in the Atmospheric Surface Layer: A Re-evaluation', *Boundary-Layer Meteorol.* **42**, 55–78.

Leslie, L. M., Mills, G. A., Logan, L. W., Gauntlett, D. J., Kelly, G. A., Manton, M. J., McGregor, J. L. and Sardie, J. M.: 1985, 'A High Resolution Primitive Equations NWP Model for Operations and Research', *Aust. Meteorol. Mag.* **33**, 11–35.

Louis, J. F.: 1979, 'A Parametric Model of Vertical Eddy Fluxes in the Atmosphere', *Boundary-Layer Meteorol.* **17**, 187–202.

Louis, J. F., Tiedtke, M., and Geleyn, J.-F.: 1981, 'A Short History of the PBL Parameterization at ECMWF', in *Workshop on Planetary Boundary Layer Parameterization*, ECMWF, Shinfield Park, Reading, Berks, U.K., 260 pp.

Mahfouf, J. F., Richard, E., Mascart, P., Nickerson, E. C., and Rosset, R.: 1987, 'A Comparative Study of Various Parameterizations of the Planetary Boundary Layer in a Numerical Mesoscale Model', *J. Clim. Appl. Meteorol.* **26**, 1671–1695.

Mahrer, Y. and Pielke, R. A.: 1977, 'A Numerical Study of the Airflow over Irregular Terrain', *Beitr. Phys. Atmosph.* **50**, 98–113.

Manins, P. C.: 1982, 'The Daytime Planetary Boundary Layer: a New Interpretation of Wangara Data', *Quart. J. Roy. Meteorol. Soc.* **108**, 689–705.

McNider, R. T. and Pielke, R. A.: 1981, 'Diurnal Boundary-layer Development over Sloping Terrain', *J. Atmos. Sci.* **38**, 2198–2212.

Mellor, G. L. and Yamada, T.: 1974, 'A Hierarchy of Turbulence Closure Models for Planetary Boundary Layers', *J. Atmos. Sci.* **31**, 1791–1806.

Nickerson, E. C., Richard, E., Rosset, R., and Smith, D. R.: 1986, 'The Numerical Simulation of Clouds, Rain and Airflow over the Vosges and Black Forest Mountains: a Meso-$\beta$ Model with Parameterized Microphysics', *Mon. Wea. Rev.* **114**, 398–414.

O'Brien, J. J.: 1970, 'A Note on the Vertical Structure of the Eddy Exchange Coefficient in the Planetary Boundary Layer', *J. Atmos. Sci.* **27**, 1213–1215.

Webb, E. K.: 1970, 'Profile Relationships: the Log–Linear Range and Extension to Strong Stability', *Quart. J. Roy. Meteorol. Soc.* **96**, 67–90.

Webb, E. K.: 1982, 'Profile Relationships in the Superadiabatic Surface Layer', *Quart. J. Roy. Meteorol. Soc.* **108**, 661–688.

Wieringa, J.: 1980, 'A Revaluation of the Kansas Mast Influence on Measurements of Stress and Cup Anemometer Overspeeding', *Boundary-Layer Meteorol.* **18**, 411–430.

Yaglom, A. M.: 1977, 'Comments on Wind and Temperature Flux-Profile Relationships', *Boundary-Layer Meteorol.* **11**, 89–102.

Yu, T.-W.: 1977, 'A Comparative Study on Parameterization of Vertical Turbulent Exchange Processes', *Mon. Wea. Rev.* **105**, 57–66.

Zhang, D. and Anthes, R. A.: 1982, 'A High-resolution Model of the Planetary Boundary Layer – Sensitivity Tests and Comparisons with SESAME-79 Data', *J. Appl. Meteorol.* **21**, 1594–1609.

Zhang, S. F., Oncley, S. P. and Businger, J. A.: 1988, 'A Critical Evaluation of the Von Karman Constant from a New Atmospheric Surface Layer Experiment', *Eighth Symposium on Turbulence and Diffusion*, Amer. Meteor. Soc., San Diego, 148–150.

Zilitinkevitch, S. S.: 1970, *The Dynamics of the Atmospheric Boundary Layer*, Hydrometeorological Publishing House, Leningrad (in Russian – English translation by C. Long), 289 pp.